Vietnam Journal of Catalysis and Adsorption
Tạp chí xúc tác và hấp phụ Việt Nam

https://jca.edu.vn

Preparation of graphene from polyethylene terephthalate (PET) bottle wastes and its use for the removal of Methylene blue from aqueous solution

Duy Khiem Nguyen[1], Thi Dung Nguyen[2], Hoang Sinh Le[1], Duong Duc La[3], Phuong Nguyen Thi Hong[4,*]

[1] *VN-UK Institute for Research and Executive Education, The University of Danang, Danang city, 550000, Vietnam*
[2] *Graduate School of Applied Chemistry, Hanyang University, Ansan 15588, Republic of Korea*
[3] *Institute of Chemistry and Materials, 17 Hoang Sam, Nghia Do, Cau Giay, Hanoi 100000, Vietnam*
[4] *School of Chemical and Life Science, Hanoi University of Science and Technology, 1 Dai Co Viet, Hai Ba Trung, Hanoi 100000, Vietnam*
**Email: phuong.nguyenthihong@hust.edu.vn*

ARTICLE INFO

Received: 20/02/2024
Accepted: 25/3/2024
Published: 30/6/2024

Keywords:
Plastic waste; graphene; polyethylene terephthalate (PET); methylene blue; adsorption

ABSTRACT

We present a method to produce graphene flakes (GFs) from polyethylene terephthalate (PET) bottle wastes by the pyrolysis method using modified bentonite as a catalyst. The as-synthesized GFs are analyzed in terms of crystal phase, morphology, and surface chemistry. The synthesized GFs have a porous, thin, and leaf-like morphology with a length ranging from a few hundred nanometers to a few tens of micrometers. The XRD and FT-IR results confirm the graphitization of PET and the presence of oxygen-containing functional groups on the surface of synthesized GFs. The obtained GFs are used as adsorbents for the removal of methylene blue (MB) from aqueous solution. The effects of various factors including, contact time, pH, and initial MB concentration, on the MB removal efficiency are examined. In addition, the adsorption isotherm models of Langmuir and Freundlich are studied. The best-fitting model is observed with the Freundlich isotherm model.

1. Introduction

Plastics are used extensively in our daily lives and have become indispensable materials of modern society owing to their excellent functional properties, durability, wide range of applications, and low cost [1]. The annual production of plastics is increasing due to the higher demand for plastics. In Vietnam, the plastics industry produced 8.89 million tons (MT) of plastic products in 2019, and approximately 2.62 MT of plastic waste is disposed of per year [2]. The accumulation of plastic wastes in landfills or oceans has caused serious environmental problems as they are mostly non-biodegradable [3]. Unfortunately, the bulk of plastic waste ends up in landfills, only 9% of plastic waste is recycled and 12% is incinerated while 22% is mismanaged and uncollected litter, causing serious environmental pollution [4,5].

Polyethylene terephthalate (PET) is one of the most widely-used plastics, mainly applied as containers in the food, beverage, and pharmaceutical industry due to its good mechanical properties, thermal stability, inertness towards food, ease of handle, transparency, and low cost [6–8]. The consumption of PET is rapidly increasing and has exceeded 24 MT/year [8]. As a consequence, large amounts of PET waste are discharged every year. This

https://doi.org/10.62239/jca.2024.030

may lead to grave environmental pollution. For many years, incineration has been a popular solution for the treatment of PET wastes. However, this method may lead to environmental pollution through the emissions of toxic compounds such as toxins [1,9]. An alternative route to eliminate PET waste is landfilling. Nevertheless, this approach may increase land used for landfilling and contaminate groundwater and soil. More seriously, the disposal of PET wastes into oceans could cause a significant threat to the health of aquatic organisms [5]. Thus, the development of new advanced technologies for recycling PET waste to maximize their utility and ensure environmental protection, is necessary.

Pyrolysis of plastic wastes has emerged as a promising recycling method that may convert plastic wastes into higher-value products. This is a process of cracking plastic waste at high temperatures in the absence of oxygen [10]. Recently, many studies on recycling of PET waste to produce high-value carbon materials using the pyrolysis technique have been reported [6–8,11,12]. In fact, PET is a good source material to be used for the synthesis of high-value carbon materials because it has a high percent of carbon (62.5%), and is free of inorganic matter [7,8,12]. The high-value carbon products synthesized from PET wastes have been used for various applications. For example, Pandey *et al.* and Karakoti *et al.* synthesized graphene nanosheets (GNs) from plastic wastes, and used them for the fabrication of dye-sensitized solar cells and supercapacitors [13,14]. Mendoza-Carrasco *et al.* prepared high-quality activated carbons (ACs) from PET bottle waste, and the obtained ACs were used as adsorbents to remove pollutants from aqueous solution [7].

In recent years, carbon-based nanomaterials have been widely used as adsorbents to remove dyes from industrial wastewaters, such as activated carbon [24], graphene oxide [25], carbon nanotubes [26,27], and graphene [6,28]. Therefore, this study aims to convert waste PET into graphene flakes (GFs) by a simple and rapid method that involves the pyrolysis of waste PET in a tube furnace using modified bentonite as a catalyst. The obtained GFs were used as adsorbents for the removal of MB from its aqueous solution. This proposed procedure has double benefits as it can reduce plastic waste and help to solve the problems of wastewater pollution.

2. Experimental

Materials

Modified bentonite was a gift from the Institute for Technology of Radioactive and Rare Elements (Hanoi City, Vietnam). Methylene blue, HCl (35%), and NaOH (98%) were obtained from Sigma-Aldrich (St. Louis, MO, USA). All aqueous solutions were prepared with deionized (DI) water generated by a water purification system (Human, Korea) at ambient conditions.

Preparation of GFs from PET plastic wastes

Figure 1 schematically illustrates the preparation process of GFs from PET plastic wastes. PET water bottle wastes were collected from domestic garbage bins and chopped into 1-3 mm pieces using a cutting machine. The chopped plastics were rinsed with DI water, dried at 105 ^{o}C for 24 h, and mixed with modified bentonite catalysts in a typical weight ratio of 10:1 [17]. The mixture was introduced into a combustion boat. The filled boat was then placed into a tube furnace (Zhengzhou KJ Technology Co., Ltd, Zhengzhou, China) and heated to 700 °C in an N_2 atmosphere (10 ml/min) with a heating rate of 10 ^{o}C/min and held for 15 min [17].

After pyrolysis, the formed product was cooled to room temperature and subsequently purified by immersing in 5% HCl solution for 3 h to remove the used catalyst and amorphous carbon residue [15]. The obtained GFs were consecutively washed with DI water by vacuum filtration and dried at 105 ^{o}C for 2 h. The final dried samples were further hand-ground in a mortar to homogenize the particles, and stored for further use.

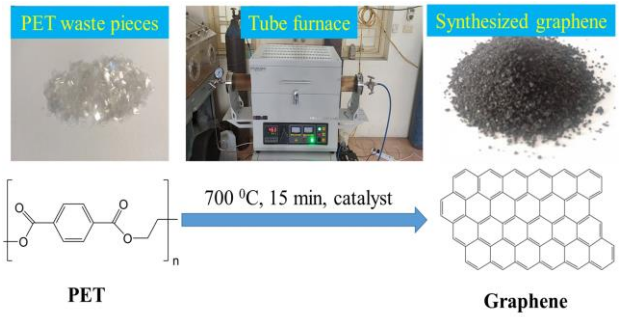

Fig. 1: Schematic illustration of the preparation process of GFs from PET plastic wastes

Characterization of the synthesized GFs

The morphology and microstructures of the samples were investigated using a scanning electron microscope (SEM) (Horiba, Kyoto, Japan). X-ray diffraction (XRD) analysis of the samples was performed on an X-ray diffractometer (Malvern Panalytical Ltd, United Kingdom) with Cu Kα radiation. UV/Vis absorption spectra of the solutions were observed using a UV/Vis spectrophotometer (Agilent, USA). The Fourier Transform Infrared (FT-IR) spectrum of the samples was measured from 400 to 4000 cm^{-1} using an FT-IR spectrometer (Perkin Elmer, USA).

https://doi.org/10.62239/jca.2024.030

The specific surface areas of the samples were analyzed using the Brunauer–Emmett–Teller (BET) method with NOVA touch 2LX instrument (Quantachrome, USA). The pH of the point of zero charge (pH_{pzc}) was determined by adding 100 mg of the prepared graphene into several vials containing 20 mL of 0.05 mol/L NaCl solution at different initial pH (ranging from 3 to 11). The initial pH (pH_i) of the solution was adjusted by using 0.01 M HCl or 0.01 M NaOH solutions. The vials were maintained at 25 °C in a shaker at an agitation speed of 200 rpm for 48 h. The final pH (pH_f) of the suspensions was measured using a pH meter. The pH_{pzc} value is the point where the pH difference (pH_f - pH_i) versus pH_i curve crosses a line equal to zero [29].

Adsorption tests

The effects of contact time, initial solution pH, and initial dye concentration on the MB dye removal efficiency were examined by a batch procedure. After adsorption, the solid residue was removed, and the UV/Vis absorbance of the supernatants was observed. The absorbance value of each sample at 664 nm (A_{664}) was determined, and the concentration of dyes was calculated using a standard calibration curve (Figure S1, Supporting Information). The adsorption capacity at t time (Q_t, mg/g), the adsorption capacity at equilibrium time (Q_e, mg/g), and the MB removal efficiency (H, %) were determined according to the reported literatures [6,20,21].

$$Q_t = (C_0 - C_t) \times \frac{V}{m} \quad (1)$$

$$Q_e = (C_0 - C_e) \times \frac{V}{m} \quad (2)$$

$$\mathrm{H} = (C_0 - C_t) \times \frac{100}{C_0} \quad (3)$$

Where C_0, C_t, and C_e (mg/L) are the MB concentrations at initial, t, and equilibrium time, respectively; V (L) is the volume of MB solution; and m (g) is the mass of synthesized graphene.

Effect of contact time: To evaluate the effect of contact time on the MB dye removal efficiency, 20 mg of GFs was mixed with 10 mL of 10 mg/L MB dye solution. The mixtures were magnetically stirred at 200 rpm at 30 °C. Solutions of 0.01 N HCl or 0.01 N NaOH were used to adjust the solution pH value until reached 7.0. At defined time points (0.5, 1, 1.5, 2, 2.5, 3, 4, 5, 7, and 10 min), the stirring was stopped, the solid residue was removed, and the absorbance of the supernatants was observed.

Effect of initial solution pH: The effect of initial solution pH on the MB dye removal efficiency was studied in a pH range of 2 – 12. An amount of 20 mg of GFs was added into 10 mL of 10 mg/L MB dye solution. Solutions of 0.01 N HCl or 0.01 N NaOH were used to adjust the solution pH. The mixtures were magnetically stirred at 200 rpm for 5 min at 30 °C. After adsorption, the solid residue was removed, and the UV/Vis absorbance of the supernatants was observed.

Effect of initial MB concentration: The effect of initial MB concentration on the MB dye removal efficiency was investigated by adding 20 mg of GFs into 10 mL of MB dye solution at different concentrations (10 – 30 mg/L). The pH of the mixtures was adjusted to 7.0 and the mixtures were magnetically stirred at 200 rpm for 5 min at 30 °C.

Adsorption isotherms

Adsorption isotherm represents the relationship between the adsorption capacity of the adsorbate (Q_e) and the adsorbate's concentration in the solution (C_e) at equilibrium and constant temperature [30]. Adsorption isotherm describes the interaction between adsorbates and adsorbents, and the distribution of adsorbate molecules between the solution and the adsorbents. Several isotherm models have been developed, but Freundlich and Langmuir isotherms are the most common models used to explain the adsorption mechanisms of various systems [31–33].

Langmuir isotherm model is based on the following assumptions: [6,20,22,31]

The linear equation of Langmuir isotherm is represented as follows:

$$\frac{C_e}{Q_e} = \frac{1}{K_L Q_m} + \frac{1}{Q_m} C_e \quad (4)$$

Where C_e (mg/L) and Q_e (mg/g) are the MB concentration and the adsorption capacity at equilibrium, respectively; Q_m (mg/g) is the maximum adsorption capacity and K_L (L/mg) is the Langmuir adsorption equilibrium constant.

The Freundlich model is an empirical equation with the assumption that the adsorbent surface is heterogeneous and contains adsorption sites. The adsorption occurs on sites with different adsorption energies depending on the coverage area [34]. The logarithmic linear equation of Freundlich isotherm is given as follows:

$$\ln Q_\mathrm{e} = \ln K_f + \frac{1}{n} \ln C_e \quad (5)$$

Where K_f is Freundlich equilibrium constant [$(mg/g)(mg/L)^{-1/n}$], and n is the heterogeneity factor [20,22].

https://doi.org/10.62239/jca.2024.030

3. Results and discussion

Characterization of the synthesized graphene

The BET surface area of the synthesized graphene was 514.34 m^2/g, which was higher than those of some other graphene materials prepared from waste biomass such as cellulose-based fiberboard (333-391 m^2/g) [35], palm kernel shell (351.26 m^2/g) [36], wheat straw (35.5 m^2/g) [37], and dead camphor leaves (296 m^2/g) [38]. The high BET surface area is very important for adsorption processes [39].

The pH of the point of zero charge (pH_{pzc}) is the pH value at which the surface electrical charge of the material is equal to zero. As shown in Fig. S2, the value of pH_{pzc} for the synthesized GFs was determined to be 6.93. Therefore, the surface of the GFs can be considered positively charged when pH < 6.93 and negatively charged when pH > 6.93.

The surface morphology of the prepared graphene is investigated via scanning electron microscope (SEM). Figure 2 presents the SEM micrographs of the prepared GFs at different magnifications. These images show a rough, thin, and leaf-like morphology of the GFs, which is useful for removing dyes from contaminated water. The length of the resultant GFs ranges from a few hundred nanometers to a few tens of micrometers. This result is in fairly good agreement with the reported results [14,17].

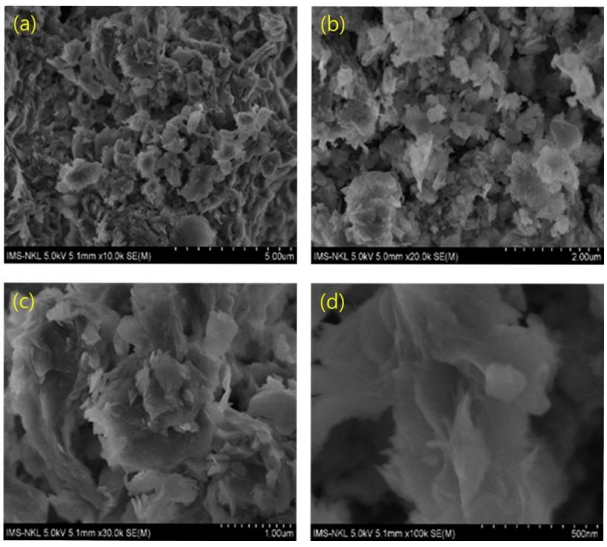

Fig. 2: SEM micrographs of the GFs at different magnifications: (a) 10k, (b) 20k, (c) 30k, and (d) 100k

Figure 3a presents the XRD pattern of the synthesized GFs. The XRD spectrum shows three sharp and narrow diffraction peaks at 2θ = 26.8°, 42.7°, and 50.2°, which are the characteristic peaks and the graphitic peaks of graphene [6,8,15,17]. The appearance of the diffraction peak at 26.8° signifies a stacking order of graphene layers [6,8]. The presence of a single peak at 42.7° suggests a low crystallinity of the synthesized GFs. All of these peaks are evidence of graphitization [8].

The FT-IR spectrum of the sample was analyzed to identify the surface functional groups of the synthesized graphene (Fig. 3b). The FT-IR spectrum showed characteristic absorption peaks corresponding to the C-O (1043 and 1454 cm^{-1}), C-C (1388 cm^{-1}), O-H (3450 cm^{-1}), aromatic C=C (1637 cm^{-1}), and C-H (2852 and 2924 cm^{-1}) stretching vibration [15,40,41]. The presence of an aromatic C=C band (1637 cm^{-1}) further confirmed the graphitization of PET by the pyrolysis method as this band is an intrinsic characteristic of sp^2 graphitic materials [42]. Moreover, the existence of the C-O band and O-H band in the FT-IR spectrum suggests that the surface of synthesized GFs was partially oxidized during the synthesis or purification steps [15]. These oxygen-containing functional groups are known as useful groups for removing dyes in water due to the interactions between these functional groups and dye molecules [6]. These findings are consistent with the reported results [6,15,17]. The FT-IR, SEM, and XRD results confirmed the formation of GFs from PET plastic waste by using our pyrolysis method in the presence of catalysts.

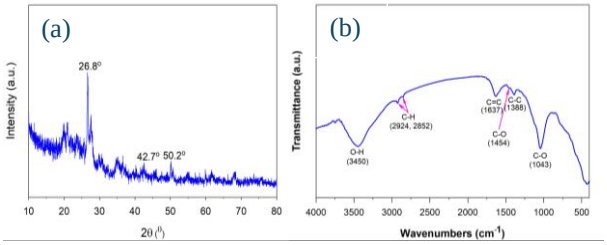

Fig. 3: (a) XRD pattern of the synthesized GFs, (b) FT-IR spectrum of the synthesized GFs

Adsorption tests

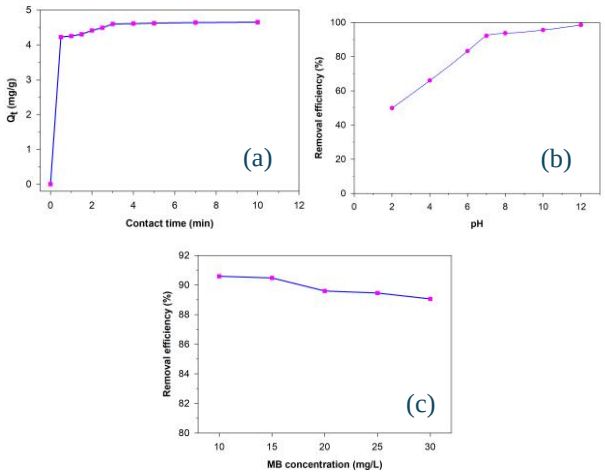

Fig .4: (a) Effect of contact time on MB adsorption, (b) Effect of pH on MB adsorption, (c) Effect of initial MB concentration on MB adsorption

https://doi.org/10.62239/jca.2024.030

Effect of contact time: As shown in Figure 4a, the adsorption capacity (Q_t) increased as the contact time increased. The Q_t value increased rapidly in the initial stage to about 4.61 mg/g, which corresponds to 92.15% MB removal efficiency. This can be explained by the porous structure of GFs, which accelerates the diffusion and adsorption of MB [43]. After this period, the Q_t value increased slowly because the number of vacant adsorption sites was reduced. Moreover, the repulsive forces between the MB molecules in the solution and those adsorbed onto GFs may decelerate the adsorption rate of MB [6]. The adsorption of MB on GFs attained equilibrium after 4 min. This result is similar to that of the previous study which used hydroxyapatite as an adsorbent to remove MB in aqueous media [31].

Effect of initial solution pH: MB is a cationic dye, which becomes positively charged ions (MB^+) in aqueous solution [32]. In this study, the synthesized graphene was used as an adsorbent, and MB dye was used as an adsorbate. The pH values of the MB solution were adjusted in the ranges of 2–12. As shown in Figure 4b, the removal efficiency of MB increased with increasing the solution pH, and the maximum MB adsorption was achieved at pH = 12. This result may be explained by the change in the surface charge of the adsorbent [31,32]. As the pH_{pzc} of the GFs is 6.93, the surface charge of GFs becomes positive (+) at pH < 6.93 and becomes more negative (-) at pH > 6.93. Therefore, at pH < pH_{pzc}, the positively charged surface of GFs inhibits the adsorption of MB^+ ions due to the repulsive forces [6,44]. Moreover, a high concentration of protons (H^+) would compete with MB^+ ions for the adsorption sites leading to a low MB removal efficiency. At pH > pH_{pzc}, the surface charge of GFs becomes more negative and the concentration of H^+ decreases, promoting MB adsorption, and leading to a high MB removal efficiency. This finding is consistent with the reported results [6].

Effect of initial MB concentration (C_{MB}): It is reported that the initial contents of dyes may influence the adsorption capacity [19,43]. In our study, C_{MB} has little influence on MB removal efficiency (Fig. 4c). The MB removal efficiency slightly decreased as the C_{MB} increased. In particular, the removal efficiency decreased from 90.59% to 89.06% as the C_{MB} increased from 10 to 30 mg/L. This result agrees with the reported results [6,31].

Adsorption isotherms

In this study, MB dye was used as adsorbate and the synthesized graphene was used as adsorbent. The Freundlich and Langmuir models were used to examine adsorption behavior. The linear fitting curves of these two models and their correlation coefficients (R^2) are shown in Fig. 5.

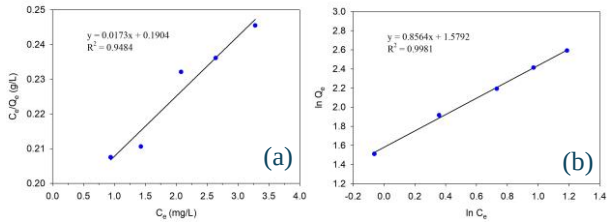

Fig. 5: (a) Langmuir plot for MB adsorption onto synthesized GFs, (b) Freundlich plot for MB adsorption onto synthesized GFs

Based on the slopes and intercepts of these curves, the isotherm parameters were determined and are listed in Table 1. According to the correlation coefficients, Freundlich isotherm is the best-fitting model due to its higher R^2 (R^2 = 0.9981). This implies that the MB adsorption onto synthesized GFs obeys the Freundlich model and proceeds by multilayer adsorption [43].

Table 1: Isotherm parameters for MB adsorption onto synthesized GFs at 30 °C

Langmuir model	K_L (L/mg)	Q_m (mg/g)	R^2
	0.091	57.80	0.9484
Freundlich model	K_f (mg/g)(mg/L)$^{-1/n}$	n	R^2
	4.851	1.168	0.9981

4. Conclusion

PET plastic waste was successfully converted into GFs via the pyrolysis method using modified bentonite as a catalyst. The modified bentonite used in the synthetic process plays an important role in shortening the synthesis procedure and reducing the maximum temperature required for the dissociation of plastic wastes. In this study, the thermal treatment was shortened to 15 min and the pyrolysis temperature was significantly reduced to 700 °C, as compared to that of the previous study synthesized graphene without catalysts at 800 °C for 1 h [6]. The adsorption capacity was significantly affected by the contact time and pH, while was negligibly influenced by the MB concentration. The MB adsorption on GFs attained equilibrium after 4 min. The maximum amount of MB adsorbed onto GFs was achieved at pH = 12. The best-fitting model was observed with the Freundlich isotherm model. This study demonstrates that the graphene prepared from PET bottle waste are promising adsorbent for removing MB from wastewater. This proposed procedure has double benefits as it can reduce plastic waste and help to solve the problems of wastewater pollution.

https://doi.org/10.62239/jca.2024.030

Acknowledgments

This work was funded by the VN-UK Institute for Research and Executive Education, The University of Danang, Danang City, Vietnam.

References

1. N. Zhou, L. Dai, Y. Lv, H. Li, W. Deng, F. Guo, P. Chen, H. Lei, R. Ruan, Chemical Engineering Journal. 418 (2021) 129412. https://doi.org/10.1016/j.cej.2021.129412
2. World Bank Group 2021, Market Study for Vietnam: Washington DC. (2021)
3. L. Yao, B. Yi, X. Zhao, W. Wang, Y. Mao, J. Sun, Z. Song, Journal of Analytical and Applied Pyrolysis. 165 (2022) 105577. https://doi.org/10.1016/j.jaap.2022.105577
4. H. Jiang, W. Liu, X. Zhang, J. Qiao, Global Challenges. 4 (2020) 1900074. https://doi.org/10.1002/gch2.201900074
5. B. Kunwar, H.N. Cheng, S.R. Chandrashekaran, Renewable and Sustainable Energy Reviews. 54 (2016) 421–428. https://doi.org/10.1016/j.rser.2015.10.015
6. N.A. El Essawy, S.M. Ali, H.A. Farag, A.H. Konsowa, M. Elnouby, H.A. Hamad, Ecotoxicology and Environmental Safety. 145 (2017) 57–68. https://doi.org/10.1016/j.ecoenv.2017.07.014
7. R. Mendoza-Carrasco, E.M. Cuerda-Correa, M.F. Alexandre-Franco, C. Fernández-González, V. Gómez-Serrano, Journal of Environmental Management. 181 (2016) 522–535. https://doi.org/10.1016/j.jenvman.2016.06.070
8. S. Ko, Y.J. Kwon, J.U. Lee, Y.-P. Jeon, Journal of Industrial and Engineering Chemistry. 83 (2020) 449–458. https://doi.org/10.1016/j.jiec.2019.12.018
9. J. Aguado, D.P. Serrano, J.M. Escola, Ind. Eng. Chem. Res. 47 (2008) 7982–7992. https://doi.org/10.1021/ie800393w
10. P.B. Dewangga, Rochmadi, C.W. Purnomo, IOP Conf. Ser.: Earth Environ. Sci. 399 (2019) 012110. https://doi.org/10.1088/1755-1315/399/1/012110
11. A. Bazargan, G. McKay, Chemical Engineering Journal. 195–196 (2012) 377–391. https://doi.org/10.1016/j.cej.2012.03.077
12. A. Esfandiari, T. Kaghazchi, M. Soleimani, Journal of the Taiwan Institute of Chemical Engineers. 43 (2012) 631–637. https://doi.org/10.1016/j.jtice.2012.02.002
13. S. Pandey, M. Karakoti, K. Surana, P.S. Dhapola, B. SanthiBhushan, S. Ganguly, P.K. Singh, A. Abbas, A. Srivastava, N.G. Sahoo, Sci Rep. 11 (2021) 3916. https://doi.org/10.1038/s41598-021-83483-8
14. M. Karakoti, S. Pandey, R. Jangra, P.S. Dhapola, P.K. Singh, S. Mahendia, A. Abbas, N.G. Sahoo, Materials and Manufacturing Processes. 36 (2021) 171–177. https://doi.org/10.1080/10426914.2020.1832680
15. S. Pandey, M. Karakoti, S. Dhali, N. Karki, B. SanthiBhushan, C. Tewari, S. Rana, A. Srivastava, A.B. Melkani, N.G. Sahoo, Waste Management. 88 (2019) 48–55. https://doi.org/10.1016/j.wasman.2019.03.023
16. M. Rahman, Z.M. Shuva, Md.A. Rahman, N. Ahmed, A. Sharmin, A.A. Laboni, M. Khan, Md.W. Islam, Md. Al-Mamun, S.C. Roy, J.K. Saha, Eur J Inorg Chem. 2022 (2022) e202200409. https://doi.org/10.1002/ejic.202200409
17. J. Gong, J. Liu, X. Wen, Z. Jiang, X. Chen, E. Mijowska, T. Tang, Ind. Eng. Chem. Res. 53 (2014) 4173–4181. https://doi.org/10.1021/ie4043246
18. J. Gong, J. Liu, Z. Jiang, X. Wen, X. Chen, E. Mijowska, Y. Wang, T. Tang, Chemical Engineering Journal. 225 (2013) 798–808. https://doi.org/10.1016/j.cej.2013.03.112
19. D.K. Mahmoud, M.A.M. Salleh, W.A.W.A. Karim, A. Idris, Z.Z. Abidin, Chemical Engineering Journal. 181–182 (2012) 449–457. https://doi.org/10.1016/j.cej.2011.11.116
20. V.O. Njoku, K.Y. Foo, M. Asif, B.H. Hameed, Chemical Engineering Journal. 250 (2014) 198–204. https://doi.org/10.1016/j.cej.2014.03.115
21. A. Valério Filho, R. Xavaré Kulman, L. Vaz Tholozan, A.R. Felkl De Almeida, G. Silveira Da Rosa, Processes. 8 (2020) 1549. https://doi.org/10.3390/pr8121549
22. A. Bazan-Wozniak, R. Wolski, D. Paluch, P. Nowicki, R. Pietrzak, Materials. 15 (2022) 3655. https://doi.org/10.3390/ma15103655
23. M. Sulak, E. Demirbas, M. Kobya, Bioresource Technology. 98 (2007) 2590–2598. https://doi.org/10.1016/j.biortech.2006.09.010.
24. N. Graham, X.G. Chen, S. Jayaseelan, Water Science and Technology. 43 (2001) 245–252. https://doi.org/10.2166/wst.2001.0096
25. M. Adel, M.A. Ahmed, M.A. Elabiad, A.A. Mohamed, Monitoring & Management. 18 (2022) 100719. https://doi.org/10.1016/j.enmm.2022.100719
26. F. Mashkoor, A. Nasar, Inamuddin, Environ Chem Lett. 18 (2020) 605–629. https://doi.org/10.1007/s10311-020-00970-6
27. A.K. Dutta, U.K. Ghorai, K.K. Chattopadhyay, D. Banerjee, Physica E: Low-Dimensional Systems and Nanostructures. 99 (2018) 6–15. https://doi.org/10.1016/j.physe.2018.01.008
28. L. Hu, Z. Yang, L. Cui, Y. Li, H.H. Ngo, Y. Wang, Q. Wei, H. Ma, L. Yan, B. Du, Chemical Engineering Journal. 287 (2016) 545–556. https://doi.org/10.1016/j.cej.2015.11.059
29. T.A. Saleh, Elsevier (2022) 99–126. https://doi.org/10.1016/B978-0-12-849876-7.00009-9
30. K. Allam, A. El Bouari, B. Belhorma, L. Bih, JWARP. 08 (2016) 358–371. https://doi.org/10.4236/jwarp.2016.83030
31. Md.T. Uddin, Md.A. Islam, S. Mahmud, Md. Rukanuzzaman, Journal of Hazardous Materials. 164 (2009) 53–60. https://doi.org/10.1016/j.jhazmat.2008.07.131
32. K. Gobi, M.D. Mashitah, V.M. Vadivelu, Chemical Engineering Journal. 171 (2011) 1246–1252. https://doi.org/10.1016/j.cej.2011.05.036
33. G.M. Walker, L.R. Weatherley, Chemical Engineering Journal. 83 (2001) 201–206. https://doi.org/10.1016/S1385-8947(00)00257-6
34. D.K. Nguyen, T. Kim, Applied Surface Science. 427 (2018) 1152–1157. https://doi.org/10.1016/j.apsusc.2017.09.020
35. L. Yu, X. Wu, Q. Liu, L. Liu, X. Jiang, J. Yu, C. Feng, M. Zhong, J Nanosci Nanotechnol. 16 (2016) 12426–12432. https://doi.org/10.1166/jnn.2016.12974
36. B. Hu, C. Huang, X. Li, G. Sheng, H. Li, X. Ren, J. Ma, J. Wang, Y. Huang, Chemical Engineering Journal. 313 (2017) 527–534. https://doi.org/10.1016/j.cej.2016.12.102
37. K. Mensah, H. Mahmoud, M. Fujii, M. Samy, H. Shokry, Biomass Conv. Bioref. (2022). https://doi.org/10.1007/s13399-022-03304-4
38. Z.-X. Han, Z. Zhu, D.-D. Wu, J. Wu, Y.-R. Liu, Metal- organic and Nano-Metal Chemistry. 44 (2014) 140–147. https://doi.org/10.1080/15533174.2013.770755